HIGHLIGHT

Synthesis of copper sulphide-based hybrid nanostructures and their application in shape control of colloidal semiconductor nanocrystals

Joanna Kolny-Olesiak

Copper sulphide is a material with low toxicity and high application potential. Colloidal synthesis allows its incorporation into hybrid nanostructures, which not only combine the properties of different materials within one nanocrystal, but also exhibit new features due to the interaction of the building blocks connected on the nanometer scale. Starting with copper sulphide seeds, such hybrid nanocrystals composed of copper sulphide and semiconductors like $CuInS_2$, $CuIn_xGa_{1-x}S_2$, Cu_2ZnSnS_4, ZnS, CdS, and PbS have been synthesized. In some of these reactions the main focus lies on the formation of new hybrid nanocrystals; in others copper sulphide plays the role of a catalyst, and copper sulphide containing hybrid nanoparticles are only intermediates in the synthesis and shape control of other semiconductor materials. Both possibilities and the underlying growth mechanisms are discussed in this article.

Introduction

The field of nanochemistry rapidly evolved during the last two decades. Synthetic procedures have been developed which allow for precise control of the size, shape, structure and composition of a variety of nanostructured materials.[1–8] These paved the way for studying the size and shape dependent properties of nano-crystallites, and therefore, increased our understanding of the properties of matter on the nanometer scale, resulting in possible creation of custom-made materials for a variety of applications.[9–12] The possibilities to manipulate and control the properties of nanocrystals can be greatly extended by generating nanoparticles composed of more than one material. These so-called hybrid nanocrystals not only combine different optical, magnetic or catalytic features within one nanostructure but also evolve with new characteristics.[13–16]

The focus of this article lies on the synthesis of semiconductor–semiconductor hybrid nanostructures which can be generated from copper sulphide seeds. Copper sulphide nanoparticles, which attract scientific attention due to their interesting properties, low toxicity and, therefore, high application potential, can be synthesized with a high degree of control over their size and shape.[17–22] $Cu_{2-x}S$ is a p-type semiconductor which can form several nonstoichiometric compounds with x ranging from 0 to 1 (hexagonal covellite CuS, orthorhombic anilite $Cu_{1.75}S$, hexagonal digenite $Cu_{1.8}S$, monoclinic djurleite $Cu_{1.94-1.97}S$, monoclinic roxbyite $Cu_{1.75}S$,

Energy and Semiconductor Research Laboratory, Department of Physics, Carl von Ossietzky University of Oldenburg, 26129 Oldenburg, Germany.
E-mail: joanna.kolny@uni-oldenburg.de; Fax: +49 441 798 3326;
Tel: +49 441 798 3261

hexagonal or orthorhombic chalcocite Cu_2S). Depending on the composition, the bandgap of $Cu_{2-x}S$ lies between 1.2 eV (for Cu_2S) and 2.0 eV (for CuS); thus, copper sulphide can absorb a large fraction of the solar spectrum, which makes it an interesting material for photovoltaic applications. Moreover, the large number of copper vacancies in the non-stoichiometric compounds and the resulting high concentration of free charge carriers lead to plasmonic absorption in the IR spectral region.[23] Furthermore, the presence of cationic vacancies and the high mobility of the cations facilitate incorporation of other cations into the copper sulphide lattice.

Because of these properties, copper sulphide is not only a material with high application potential but also a suitable catalyst which facilitates growth and enables shape control of other semiconductor nanomaterials. Therefore, two aspects will be discussed here: the possibility to modify the properties of copper sulphide particles by combining them with other semiconductors and the potential to synthesize shape-controlled nanocrystals in procedures including copper sulphide containing intermediates. Recent advances in the synthetic methods using copper sulphide seeds are summarized, and an overview of the current understanding of the underlying reaction mechanisms is given.

Overview of synthetic procedures

Several materials have already been combined with copper sulphide to form hybrid nanostructures, *e.g.*, $CuInS_2$,[24–28] $CuIn_xGa_{1-x}S_2$,[29,30] Cu_2ZnSnS_4,[31,32] ZnS,[33–36] CdS,[37] PbS,[38] and MnS.[39] In all cases the synthetic procedures start with the

Table 1 Overview of synthetic methods to obtain copper sulphide based hybrid nanostructures

Precursors, ligands, and solvents	Method/conditions	Shape, size, and structure	Ref.
Cu–In–S			
Cu-oleate, In-oleate, OLAM, 1-DDT	230–250 °C, 10 min - 1 h, heat-up	Acorn-shape: 30 nm × 48 nm, bottle-shape: 40 nm × 110 nm, larva-shape: 45 nm × 185 nm	Choi et al. 2006 (ref. 46)
Cu(acac)$_2$, In(acac)$_3$, 1-DDT,	200 °C, injection of In(acac)$_3$ into preformed copper sulphide seeds	HNRs: 77 nm × 12.0 nm, tear-drops: 48 nm × 23 nm	Han et al. 2008 (ref. 40)
Cu-oleate, In-oleate, 1-DDT, OLAM	215–300 °C, 20 min, heat-up	Nanorods, WZ	Connor et al. 2009 (ref. 24)
Cu(OAc)$_2$, In(OAc)$_3$, 1-DDT, t-DDT, TOPO, OLAM	240 °C, 30 s - 1 h, hot-injection	Various sizes, HNRs, P-shaped, hexagonal plates, WZ	Kruszynska et al. 2010 (ref. 25)
Cu(OAc)$_2$, In(OAc)$_3$, 1-DDT, t-DDT, TOPO, ODE, OLAM	240 °C, 50 s - 1 h, hot-injection	Triangular pyramids, WZ	Kruszynska et al. 2011 (ref. 27)
Cu(NO$_3$)$_2$, In(NO$_3$)$_3$, 1-DDT, OLAM, OA	240°, 30 min, heat-up	Quasi-spherical, rods, WZ	Lu et al. 2011 (ref. 28)
Cu(dedc)$_2$, Cu(acac)$_2$, In(dedc)$_3$, OLAM, 1-DDT	The mixture is rapidly heated to 180 °C by immersion in an oil bath, 60 min	Nanoribbons with a rectangular cross-section: 2–3 μm in length, 20–50 nm in width, 15 nm in thickness, WZ	Li et al. 2013 (ref. 29)
Cu–In–Zn–S			
CuOAc, In(OAc)$_3$, zinc stearate, zinc ethylxanthate, 1-DDT, ODE	240 °C, slow precursor injection via a syringe pump	Various sizes, Cu$_2$S–ZnS, Cu$_2$S–CIS and Cu$_2$S–(CIS–ZnS alloy) HNRs, chalcocite and WZ	Chang and Cheng 2011 (ref. 26)
Cu$_{1.94}$S–ZnS seeds, In(OAc)$_3$, 1-DDT, ODE	200 °C, 4 h, heat-up	Burning torch-like CIS–ZnS HNRs, head: 33 nm × 24 nm, tail: 29 nm × 9 nm, WZ	Yi et al. 2013 (ref. 47)
	200 °C, 6 injections of In(ac)$_3$, 4 h reaction after last injection	Long rod-like CIS–ZnS HNRs, WZ	
Cu–Zn–S			
Cu(acac)$_2$, Zn(acac)$_2$, 1-DDT	200 °C, ca. 4–5 h, injection of Zn(acac)$_2$ in 6 portions	HNRs	Yi et al. 2010 (ref. 33)
CuI, Zn(dedt)$_2$, OLAM	150 °C, 30 min, heat-up	Hexagonal prism length: 60 nm; diameter: 30 nm, monoclinic Cu$_{1.94}$S, WZ ZnS	Han et al. 2012 (ref. 35)
Cu-oleate, 1-DDT, OLAM	220 °C, 30 min, injection of Zn-oleate at 220 °C	28 nm slab-like ZnS nanocrystals embedded in a Cu$_{1.94}$S nano-sphere, monoclinic Cu$_{1.94}$S and WZ ZnS	Huang et al. 2012 (ref. 34)
Zn(acac)$_2$, Cu(acac)$_2$, 1-DDT, ODE	240–270 °C, reaction times up to 360 min, heat-up	Taper-like, matchstick-like, tadpole-like, or rod-like hybrid nanostructures, monoclinic Cu$_{1.94}$S, WZ ZnS	Ye et al. 2013 (ref. 36)
Cu–In–Ga–S			
Cu(acac)$_2$, In(acac)$_3$, Ga(acac)$_3$, TOPO, ODE, 1-DDT, t-DDT	Injection at 155 °C, reaction temperature: 250–270 °C, 15–30 min	Nanorods, diameter: 7 nm, WZ	Coughlan et al. 2013 (ref. 30)
Cu(dedc)$_2$, Cu(acac)$_2$, In(dedc)$_3$, Ga(dedc)$_3$, OLAM, 1-DDT	The mixture is rapidly heated to 180 °C by immersion in an oil bath, 60 min	Nanoribbons with a rectangular cross-section: 1–2 μm in length, 30–50 nm in width, 9 nm in thickness, variable composition between 20 and 80% Ga, roxbyite and WZ	Li et al. 2013 (ref. 29)
Cu–Zn–Sn–S			
Cu(acac)$_2$, Zn(OAc)$_2$, SnCl$_2$, 1-DDT, OLAM,	200–260 °C, different reaction times: up to 24 h, heat-up	Bullet-shape, 13 nm, WZ	Liao et al. 2013 (ref. 32)
CuCl$_2$, Zn(dedc)$_2$, Sn(dedc)$_4$, 1-DDT, OLAM	200 °C, 60 min, fast heat-up by immersion in an oil bath	Nanorods, 200 nm in length, WZ	Zhang et al. 2013 (ref. 31)
Cu–Cd–Zn–S			
Cu(dedt)$_2$, Cd(dedt)$_2$, Zn(dedt)$_2$ hexanethiol, trioctylamine	250 °C, injection of Cd(dedt)$_2$ and Zn(dedt)$_2$ into preformed Cu$_{1.94}$S seeds	Hexagonal discs with regions of monoclinic Cu$_{1.94}$S and WZ CdS (Cd$_x$Zn$_{1-x}$S)	Regulacio et al. 2011 (ref. 37)
Cu–Pb–S			
Cu(acac)$_2$, Pb(dedt)$_2$, 1-DDT	200 °C, 10 min, injection of Pb(dedt)$_2$ into preformed Cu$_{1.94}$S seeds	HNRs, chalcocite and rock salt	Zhuang et al. 2012 (ref. 38)
Cu–Mn–S			
Cu(OAc)$_2$, Mn(OAc)$_2$ 1-DDT, OLAM	220 °C, 15 min, injection of Mn(ac)$_2$ into preformed Cu$_{1.94}$S seeds	HNRs, 16 nm in length, djurleite and WZ	Zhou et al. 2013 (ref. 39)

acac: acetylacetonate, dedt: diethyldithiocarbamate, 1-DDT: 1-dodecanethiol, t-DDT: tert-dodecanethiol, HDA: hexadecylamine, HNRs: hetero-structured nanorods, OA: oleic acid, OAc: acetate, ODE: octadecene, OLAM: oleylamine, TOPO: trioctylphosphine oxide, WZ: wurtzite, and ZB: zincblende.

formation of copper sulphide seeds, which subsequently react with other cations and an additional sulphur source to form heterostructured nanocrystals. These two steps can follow each other in a one-pot (heat-up or hot-injection)

reaction; differences in the reactivity of the cations forming both parts of the nanostructure are in many cases sufficient to separate these two stages of the synthesis. Other procedures use preformed seeds (usually in the original reaction solution without further purification), and the formation of the hybrid nanoparticles is induced by the addition of the precursors for the formation of the second semiconductor material.[37–40] New educts can be added all at once, in several small injections or continuously using a syringe pump. The rate of the addition of the precursors can influence the morphology of the resulting nanocrystals; other parameters, which can be varied to control the size and the shape of the resulting nanocrystals are the ratio between copper and the other cations and the reaction temperature. Experimental details of the synthesis of different copper sulphide based heterostructured nanocrystals as well as information about the morphology of the resulting materials can be found in Table 1.

Growth mechanisms

Although all of the synthetic methods described here follow a similar general pathway, they differ in the underlying growth mechanism (see Scheme 1). Most of the studies discussed in the next section describe the formation of one-dimensional hybrid nanocrystals. This kind of structure can be generated
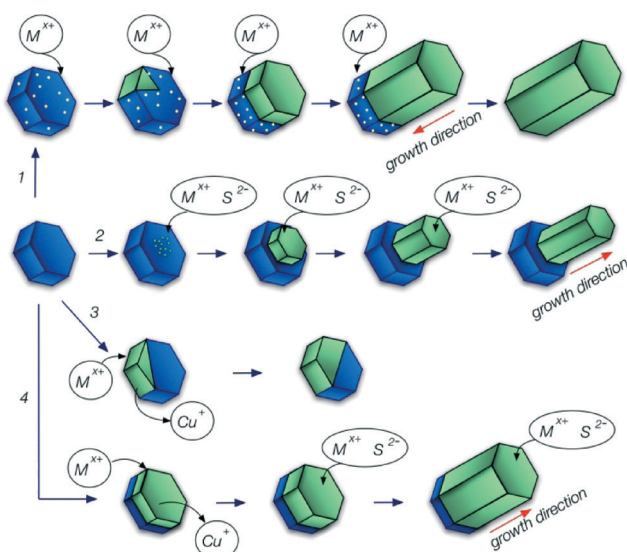
Scheme 1 Possible growth mechanisms of copper sulphide based hybrid nanostructures by reaction with other cations M^{x+} (In^{3+}, Ga^{3+}, Zn^{2+}, Sn^{2+}, Cd^{2+}, Pb^{2+}, or Mn^{2+}). Pathway 1: copper sulphide plays the role of a catalyst. Dissolution of M^{x+} in the copper sulphide phase leads to the nucleation of a second semiconductor material. The growth takes place at the interface between the two phases. In some cases the copper sulphide phase gradually disappears. Pathway 2: copper sulphide plays the role of a seed for heterogeneous nucleation of another material on its surface; the resulting particles are always copper sulphide containing heterostructures. Pathway 3: partial cation exchange leading to the formation of copper sulphide containing heterostructures. Pathway 4: partial cation exchange followed by seeded growth.

by two mechanisms: seeded growth or catalyst assisted growth. In both cases the synthesis starts with the formation of particles, which subsequently serve as starting points for the growth of another material. However, the role of these seeds in the growth process of the second material is different for both mechanisms.

In seeded growth a second material nucleates on the surface of the first one. Its further growth takes place directly through accretion of monomers from solution, without any additional contribution from the original seed and the growth direction is away from the original seed (see Scheme 1 pathway 2).

In catalyst assisted growth, usually materials with a relatively low melting point (e.g., Au, Bi, In or Sn) are used as catalysts. The precursors of the second material dissolve in the liquid catalyst, but because of its limited solubility, above some critical concentration the second material forms a solid seed inside the first one, which subsequently grows through addition of monomers dissolved in the catalyst (see Scheme 1 pathway 1). This method has been effectively used to produce nanorods and nanowires of many different materials starting with precursors in the gas phase (vapour–liquid–solid procedure) or in solution (solution–liquid–solid procedure).[41,42]

Also copper sulphide can play the role of a catalyst in the growth of other materials, in spite of being solid at the reaction temperatures typically used in colloidal synthesis. Copper sulphide is a solid-state superionic conductor.[43–45] At a relatively low temperature of 105 °C Cu_2S undergoes phase transformation to a solid–liquid hybrid phase: the copper cations move like a liquid through the anion sublattice, which maintains its solid form.[45]

The sulphur anion sublattice of Cu_2S is nearly identical to that of other metal sulphides with a wurtzite structure, e.g., $CuInS_2$, $CuGaS_2$, Cu_2ZnSnS_4, MnS or ZnS (see Fig. 1 for a comparison of the Cu_2S and $CuInS_2$ structures). Therefore, in most cases materials growing via a route involving hybrid structures with copper sulphide exhibit a wurtzite structure, even if this is not the thermodynamically stable modification at room temperature.

In some of the examples discussed below the formation of a hybrid nanostructure involves cation exchange.[37–39] This method can be used when both materials involved contain
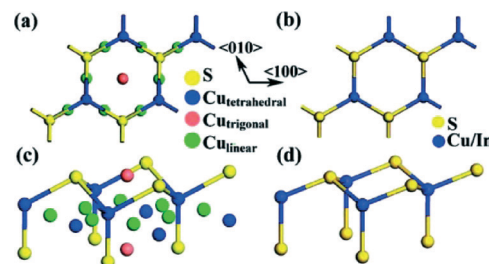

Fig. 1 Crystal structures of (a) hexagonal chalcocite Cu_2S and (b) hexagonal $CuInS_2$ with a zone axis of ⟨001⟩. Crystal structures of (c) hexagonal chalcocite Cu_2S and (d) hexagonal $CuInS_2$ viewed from another angle. Reprinted with permission from J. Am. Chem. Soc., 2009, **131**, 4962–4966. Copyright (2009) American Chemical Society.

the same kind of anion while the cations possess different chemical properties.

When hybrid nanostructures are formed through this mechanism, only part of the seed undergoes cation exchange (Scheme 1 pathway 3). Usually, during cation exchange the anion lattice does not change,[48] therefore the resulting particles retain the shape of the original seeds.

The next growth mechanism, suggested for MnS and some of the ZnS containing hybrid nanostructures, also involves cation exchange but only in the initial step of the formation of the hybrid nanocrystal. After the formation of a hybrid nanostructure due to partial cation exchange the further growth follows the same pathway as that for the seeded growth described above (Scheme 1 pathway 4).

Overview of hybrid nanostructures with copper sulphide

Ternary and quaternary copper sulphides

Nanoparticles composed of ternary and quaternary copper sulphides, such as copper indium sulphide, copper gallium sulphide and copper zinc tin sulphide, are of particular interest as absorber materials for solar energy conversion.[7,8,49] Controlling the size, shape, structure and composition of these nanoparticles is essential to fully exploit their application potential. Therefore, there is a lot of activity in the field of colloidal synthesis of these nanocrystalline semiconductors. One possible way to control their shape is to use copper sulphide based intermediates in the synthesis. The following paragraphs give a short overview of the development of the synthetic methods for colloidal $CuInS_2$, $CuGaS_2$, $CuIn_xGa_{1-x}S_2$ and Cu_2ZnSnS_4 nanocrystals using this approach.

The first example of shape-controlled hybrid nanostructures containing a copper sulphide phase was published in 2006 by Choi et al.[46] (Fig. 2). Cu_2S was generated in the beginning of a one-pot heat-up reaction in a decomposition process of copper oleate and dodecanethiol, yielding oleic acid and dodecene as by-products.

The subsequent formation of the hybrid nanoparticles was described as seed-mediated growth of a second phase on the surface of the Cu_2S particles. The X-ray diffraction (XRD) pattern of the resulting particles was assigned to a mixture of the tetragonal structure of In_2S_3 and the hexagonal chalcocite-structured Cu_2S. Spatially resolved energy dispersive X-ray analysis (EDX) measurements presented in the article show indeed the presence of copper sulphide regions within these particles; however the stoichiometry of the resulting particles is close to $1:1:2$ (Cu : In : S), which gives rise to the assumption that it is composed of copper indium disulphide and not indium sulphide. This is further supported by the comparison of the diffraction data presented within the article with the diffraction patterns of wurtzite copper indium disulphide (first described in 2008 by Pan et al.[50]). The reflections assigned to Cu_2S–In_2S_3 match exactly the positions of the reflections of wurtzite copper indium disulphide. Also a comparison with the XRD data of other copper sulphide containing heterostructures[26,27,31,38]
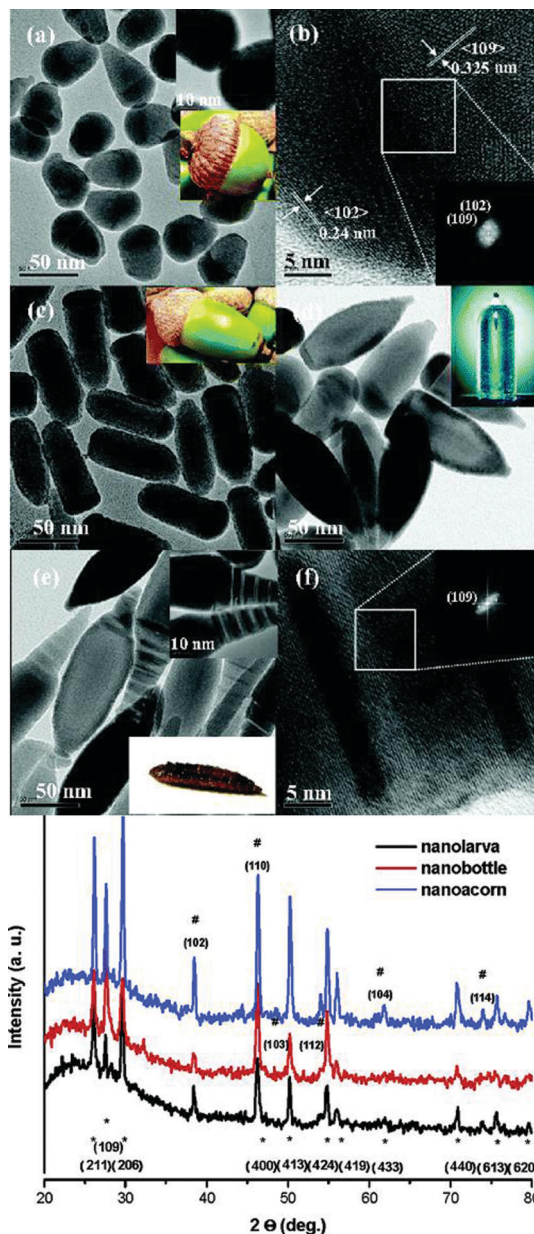

Fig. 2 (a) A TEM image of short nanoacorns (inset: enlarged image). (b) An HRTEM image of short nanoacorns (inset: an FFT image). (c) A TEM image of long nanoacorns. (d) A TEM image of nanobottles. (e) A TEM image of nanolarvae. (f) An HRTEM image (inset: an FFT image) of nanolarvae. The lower panel shows the corresponding XRD patterns. Asterisks (*) and number signs (#) indicate the peaks from In_2S_3 (JCPDS * 73-1366) and Cu_2S (JCPDS # 84-0206), respectively. Adapted with permission from *J. Am. Chem. Soc.*, 2006, **128**, 2520–2521. Copyright (2006) American Chemical Society.

shows that the intensity of the reflections, which can be assigned to the copper sulphide phase, is usually relatively low compared to that of, e.g., $CuInS_2$ (see Fig. 3). Therefore, the interpretation of the data presented in the article, especially the assignment of the phases, should probably be partly reconsidered.

A study presenting the formation of copper sulphide/indium sulphide hybrid structures was published in 2008 by
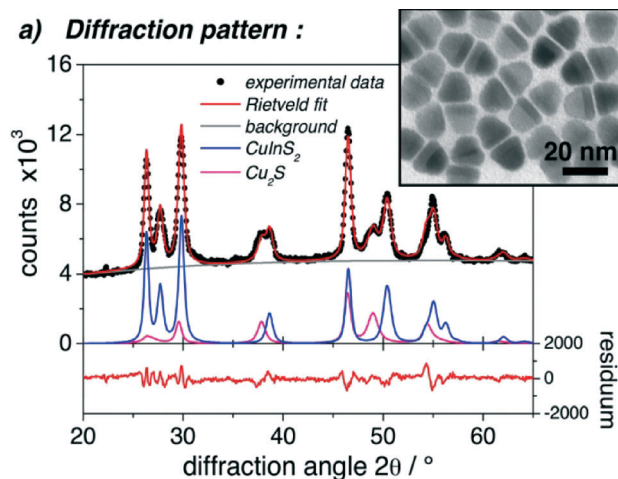
Fig. 3 Experimental XRD data for CuInS₂–Cu₂S nanoparticles (the TEM image is shown in the inset) together with the results of Rietveld refinement showing the contributions of the CuInS₂ and Cu₂S phases to the diffraction pattern. Adapted with permission from *J. Am. Chem. Soc.*, 2010, **132**, 15976–15986. Copyright (2010) American Chemical Society.

Han *et al.*[40] A high degree of shape control was achieved here by the addition of indium acetylacetonate to preformed copper sulphide seeds. By changing the time and the frequency of the addition of the indium precursor matchstick- and tear drop-like particles were synthesized. The underlying growth mechanism was investigated in this study, revealing that the formation of the hetero-nanostructures is based on a catalyst assisted mechanism rather than seed-mediated growth. However, here the assignment of the two phases comprising the hybrid nanoparticles to Cu_2S–In_2S_3 based on the XRD data might also need reconsideration because the positions of the reflections exactly match those of wurtzite copper indium disulphide.

In 2009 Connor *et al.*[24] described the synthesis of $CuInS_2$ nanorods, which starts with the formation of copper sulphide nanoparticles and goes through an intermediate stage of heterostructured $CuInS_2$–Cu_2S nanorods (Fig. 4). The crystallographic structure of the $CuInS_2$ part of the hybrid

nanostructure was identified as wurtzite. A comparison with the reference XRD data for Cu_2S and In_2S_3 clearly showed that the diffraction pattern of the particles described in the article cannot be satisfactorily explained as a superposition of the diffraction patterns of Cu_2S and In_2S_3 (see Fig. 5). Connor *et al.*[24] assumed an epitaxial growth of $CuInS_2$ on the surface of Cu_2S, followed by a phase conversion of the Cu_2S part of the hybrid structure to $CuInS_2$. The one dimensional growth of the $CuInS_2$ phase was explained by the different reactivity of the two (001) faces of the Cu_2S nanodiscs: one terminated with cations, the other with anions. At later stages of the reaction, when most of the copper precursor in the reaction solution was used up, the copper sulphide part of the nanostructure abruptly disappeared, which the authors attribute to a solid–solid seed based transformation due to the diffusion of indium ions from $CuInS_2$ to Cu_2S, facilitated by the high mobility of the cations in the copper sulphide phase at the reaction temperature. Thus, the reaction mechanism suggested here involves first epitaxial growth, while the high ionic conductivity of copper sulphide plays a role only during the last stage of the reaction.

The following articles about the synthesis $CuInS_2$ nanoparticles starting with copper sulphide seeds reported a
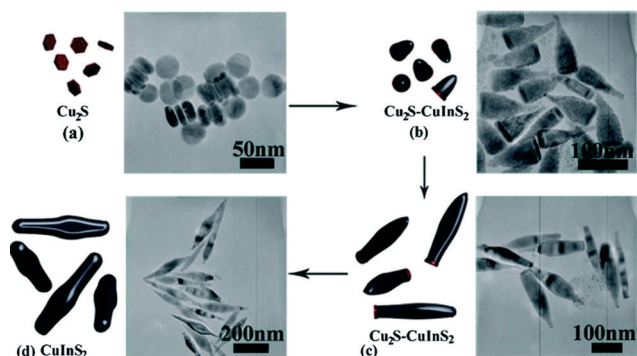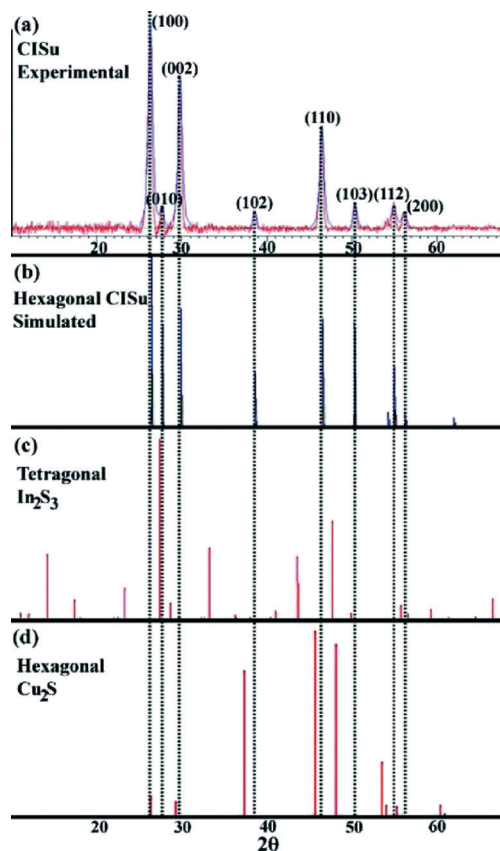

Fig. 4 Growth mechanism proposed for the formation of $CuInS_2$ nanorods. Reprinted with permission from *J. Am. Chem. Soc.*, 2009, **131**, 4962–4966. Copyright (2009) American Chemical Society.

Fig. 5 Comparison of the experimental XRD pattern of $CuInS_2$ nanorods (a) with a simulated pattern of wurtzite $CuInS_2$ (b) and reference data for In_2S_3 (c) and Cu_2S (d). Reprinted with permission from *J. Am. Chem. Soc.*, 2009, **131**, 4962–4966. Copyright (2009) American Chemical Society.

higher degree of shape control and also contributed to a better understanding of the growth process of $CuInS_2$–Cu_2S hybrid nanocrystals. In 2010 Kruszynska et al.[25,27] showed the formation of $CuInS_2$–Cu_2S and $CuInS_2$ nanorods with different aspect ratios, dimeric nanorods as well as hexagonal discs and P-shaped particles in a hot-injection synthesis (Fig. 6). Also the formation of alloyed ZnS–$CuInS_2$ nanorods was reported for the first time. The investigation of the growth process revealed that the formation of the $CuInS_2$ phase takes place inside the copper sulphide seeds. The initial quasi-spherical hybrid nanostructure evolves into a

Janus particle composed of two discs when the size of the $CuInS_2$ phase exceeds a certain size. The further growth of the $CuInS_2$ part of the hybrid nanostructure takes place only at the interface between the two phases, enabling efficient shape control of the evolving structure by influencing the size and the position of the copper sulphide phase within the hybrid structure. The copper sulphide phase disappears at the later stages of the reaction, which also stops the further growth of the $CuInS_2$ phase; this additionally supports the catalytic role of copper sulphide in this synthesis.

Lu et al.[28] published in 2011 a heat-up synthesis of $CuInS_2$ nanorods allowing for precise shape control. Here, the formation of Cu_2S in the beginning of the reaction was also assumed to play a major role in the size and shape evolution of the products of the reaction; however, no detailed investigation of the growth process was presented.

Chang and Cheng[26] synthesized particularly uniform $CuInS_2$–Cu_2S, $(ZnS)_{1-x}(CuInS_2)_x$–Cu_2S and ZnS–Cu_2S heterostructured nanorods by dropwise addition via a syringe pump of indium and/or zinc precursors to a solution of Cu_2S seeds. The growth process and the shape evolution of the hybrid nanorods were monitored by taking aliquots from the reaction solution at different reaction times and studying them by TEM and XRD (see Fig. 7); however, no proof of the suggested seeded-growth mechanism was obtained.

Not only isolated copper sulphide nanocrystals but also those already part of a heterostructure can be used to synthesize $CuInS_2$. A reaction of ZnS–Cu_2S nanorods with an indium precursor leads to the formation of $CuInS_2$–ZnS hybrid nanorods.[47] The morphology of the $CuInS_2$ part of the resulting
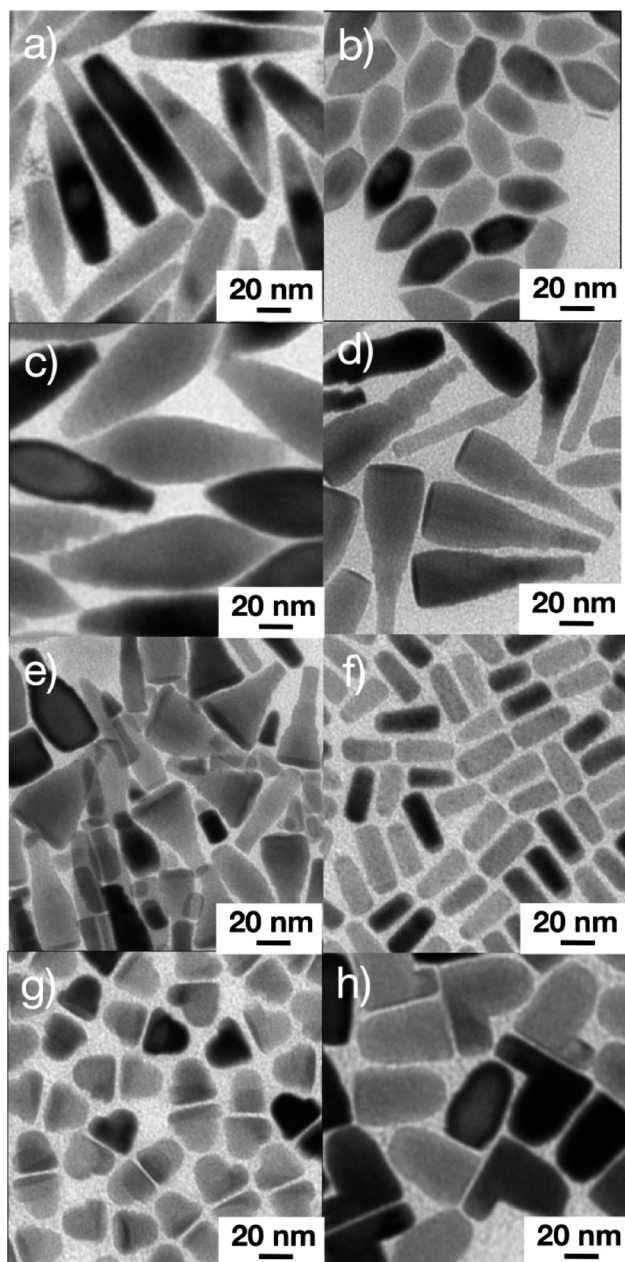

Fig. 6 Different shapes of $CuInS_2$ nanocrystals (a–d) and $CuInS_2$–Cu_2S heterostructures (e–f). Adapted with permission from J. Am. Chem. Soc., 2010, 132, 15976–15986. Copyright (2010) American Chemical Society.

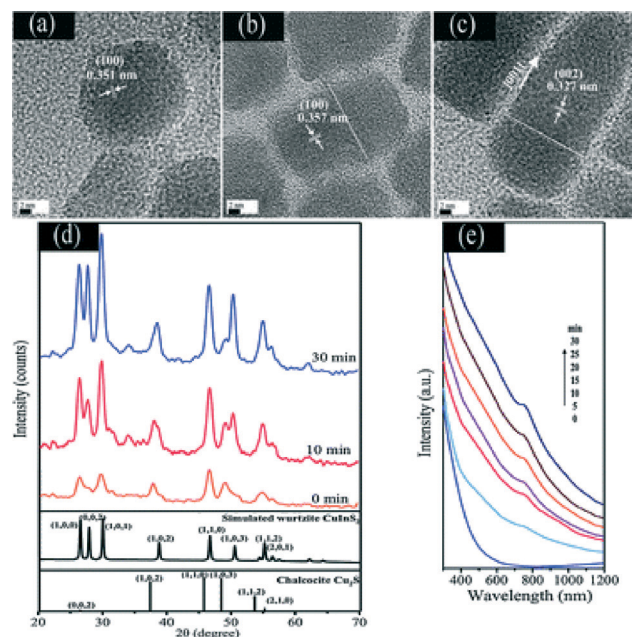Fig. 7 HRTEM images of as-prepared Cu_2S–$CuInS_2$ nanocrystals at different reaction times: (a) 0 min, (b) 10 min, and (c) 30 min. XRD patterns (d) and absorption spectra (e) of Cu_2S–$CuInS_2$ nanocrystals synthesized at different reaction times. Reproduced from ref. 26 with permission from The Royal Society of Chemistry.

nanostructures depends on the rate of the addition of the indium salt.

Another example showing the potential of copper sulphide seeds to control the shape of CuInS$_2$ and CuIn$_x$Ga$_{1-x}$S$_2$ nanocrystals was demonstrated by Li *et al.* in 2013.[29] 2–3 µm long wurtzite CuInS$_2$ and CuIn$_x$Ga$_{1-x}$S$_2$ nanoribbons with a rectangular cross-section growing along the [110] direction and enclosed by (001) and (1–10) crystallographic faces were obtained by rapidly heating the reaction mixture (Fig. 8). The growth process starts with the formation of roxbyite nanocrystals, which are subsequently converted to bat-like heterostructures with a hemispherical copper sulphide head. The

Fig. 8 TEM images of CuInS$_2$ nanoribbons. (a) The boxed parts refer to the head tip of the ribbons and the circled parts refer to the tail tip of ribbons. (b) XRD patterns of the CuInS$_2$ nanoribbons. (c) A HRTEM image of CuInS$_2$ nanoribbons. The inset shows the FFT pattern. (d) A HRTEM image of the head and body of a CuInS$_2$ nanoribbon. (e) EDS spectra collected from the head and body of CuInS$_2$ nanoribbons. (f and g) The two corresponding FFT patterns of the head and body of the nanoribbon in (d). The circled and boxed spots represent the relative orientation in Cu$_{1.75}$S and CuInS$_2$, respectively. (h) A cross-sectional HRTEM image of CuInS$_2$ nanoribbons. The inset shows the low magnification TEM image displaying a rectangular cross section. (i) The schematic morphology of the nanoribbon with the crystallographic orientation. Reproduced from ref. 29 with permission from The Royal Society of Chemistry.

roxbyite head is about 10–15 nm in diameter in the beginning of the reaction; however, it grows to 20–40 nm within the first few minutes of the synthesis after which it remains stable in size. This behavior can be attributed to catalyst swelling, *i.e.*, dissolution of In and/or Ga ions in the catalyst. Different lattice mismatch between roxbyite and wurtzite CuInS$_2$ (or CuIn$_x$Ga$_{1-x}$S$_2$) along different crystallographic directions leads to the formation of nanoribbons with a rectangular cross-section (20–50 nm: width; 15 nm: thickness). CuIn$_x$Ga$_{1-x}$S$_2$ nanorods were synthesized by a hot-injection method by Coughlan *et al.*[30] in 2013. The growth of the CuIn$_x$Ga$_{1-x}$S$_2$ nanocrystals starts with the formation of copper sulphide particles (described as a mixture of different structures: chalcocite, covellite, anilite) which are converted to CuInS$_2$ within the first 5 min of the reaction. Only during further heating do these particles react with the Ga ions present in the reaction solution to form CuIn$_x$Ga$_{1-x}$S$_2$ nanocrystals. This difference in the reactivity between indium and gallium ions can be rationalized by taking into account that Ga^{3+} is a harder acid compared to In^{3+}. The reaction conditions and stabilizers were systematically varied within this study, allowing the control of the shape of the resulting CuIn$_x$Ga$_{1-x}$S$_2$ nanocrystals. For instance, the size of the copper sulphide nanocrystals was controlled by the addition of amines with different chain lengths. In this way the diameter of the resulting nanorods could also be controlled.

Another quaternary material, which can be synthesized starting with copper sulphide seeds is wurtzite Cu$_2$ZnSnS$_4$. Liao *et al.*[32] described the formation of bullet-like Cu$_2$ZnSnS$_4$ nanocrystals from djurleite copper sulphide nanoparticles. The characterization of the reaction products obtained after different reaction times revealed that the fraction of copper sulphide within the hybrid nanostructures gradually decreased and at longer reaction times pure Cu$_2$ZnSnS$_4$ nanocrystals were obtained. Zhang *et al.*[31] synthesized leaf-shaped wurtzite Cu$_2$ZnSnS$_4$ nanoparticles 200 nm in length using cubic α-Cu$_2$S nanocrystals as a catalyst in a heat-up reaction. Nanorods with heads composed of copper sulphide were observed as an intermediate state, but the final product was pure Cu$_2$ZnSnS$_4$ due to interdiffusion of Zn, Sn and Cu between Cu$_2$ZnSnS$_4$ and Cu$_2$S.

Binary sulphides

This section is focused on the synthesis of hybrid nanostructures composed of copper sulphide and binary semiconductors, such as ZnS, CdS, PbS and MnS. The main motivation to generate this kind of hybrid nanomaterial is given by the possibility to modify the properties of copper sulphide nanocrystals in order to meet specific requirements of applications such as, photovoltaics, optoelectronics or theranostics. Copper sulphide–cadmium sulphide hetero-nanostructures have a type II band alignment, which facilitates the separation of light induced charge carriers. Therefore, this material combination is a potential absorber for nano-structured solar cells. Also the combination of copper sulphide with lead
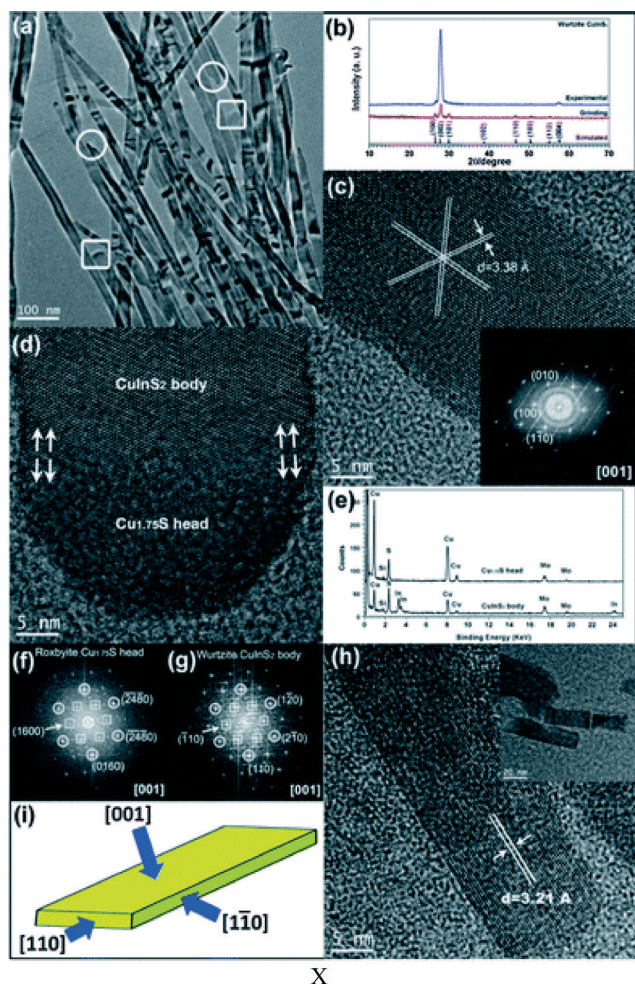
sulphide or the less toxic zinc sulphide is thought to be advantageous for applications in solar energy conversion.

Copper sulphide particles exhibit localized surface plasmon resonance due to the large number of copper vacancies, and, consequently, high concentration of free charge carriers. This feature is of interest not only from the point of view of basic research, but also for a variety of applications, *e.g.*, in photothermal therapy or as nano-antennas. The position of the plasmon band of copper sulphide particles can be influenced by combining copper sulphide with other materials, *e.g.*, ZnS or MnS. In this way custom-made plasmonic materials can be obtained, *e.g.* absorbing within the so-called "therapeutic window" (700–1500 nm) or in the wavelength range, which is of interest for applications in telecommunication devices (1200–1600 nm). Using MnS for the modification of the plasmonic absorption of copper sulphide particles shifts the absorption to the "therapeutic window" and, thus, enables the use of the resulting hybrid nanostructures in photothermal therapy. Furthermore, MnS is a paramagnetic material which can be used as a contrast agent for nuclear magnetic resonance imaging. Therefore, copper sulphide–manganese sulphide heterostructures are potential theranostic agents.

The first example of heterostructured $Cu_{1.94}S$–ZnS nanorods was presented in 2010 by Yi *et al.*[33] A Zn precursor was injected in six portions within several hours into a solution containing djurleite seeds. The thickness of the nanorods could be controlled by the size of the copper sulphide particles. The shape evolution of the ZnS nanorods indicates that the copper sulphide particles do not only serve as a template but also play the role of a catalyst in the formation of the ZnS phase.

An impressive example of shape control in a one-pot heat-up reaction was demonstrated by Han *et al.*[35] in 2012, who obtained hexagonal-prismatic $Cu_{1.94}S$–ZnS, $Cu_{1.94}S$–ZnS–$Cu_{1.94}S$, and $Cu_{1.94}S$–ZnS–$Cu_{1.94}S$–ZnS–$Cu_{1.94}S$ heteronanostructures with screw-, dumbbell- and sandwich-like shapes (Fig. 9a). The ratio between copper and zinc in the reaction solution strongly influenced the growth process and, thus, the shape of these nanostructures. Their formation was a consequence of several different growth steps, such as partial cation exchange, growth through accretion of monomers from solution and restructuring. The reaction pathways leading to the generation of different shapes are summarized in Fig. 9b.

The first study of the applicability of a $Cu_{1.94}S$–ZnS heterostructure as a nano-antenna was published in 2012 by Huang *et al.*[34] The formation of the hybrid nanoparticles was induced by the injection of a zinc precursor into preformed copper sulphide seeds. The formation of the ZnS phase embedded in copper sulphide (Fig. 10) is assumed to be due to a partial cation exchange, which is followed by the further growth outside the copper sulphide seeds by accumulation of ions from solution.

Another example of a copper sulphide–zinc sulphide nanostructure was shown in 2013 by Ye *et al.*,[36] who studied the influence of the copper to zinc ratio on the structure and the composition of the resulting particles. Copper sulphide
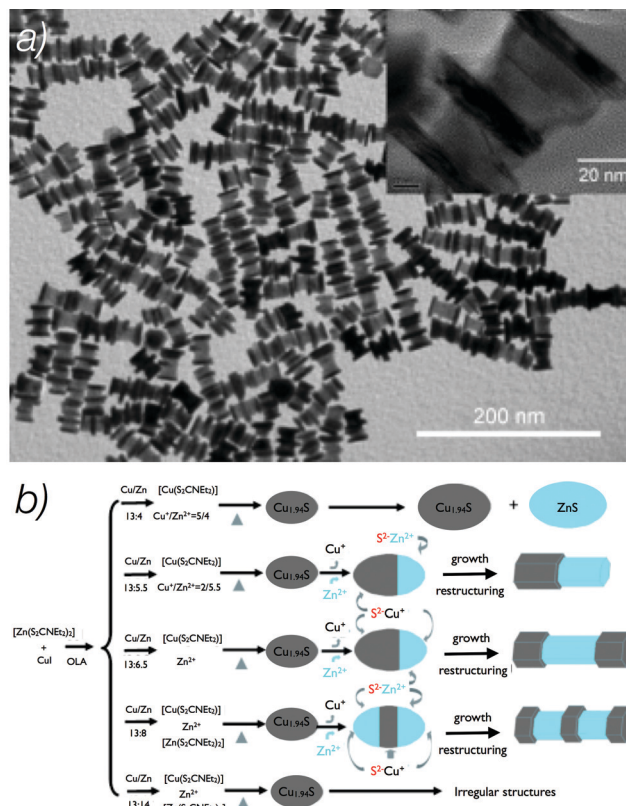

Fig. 9 TEM image of $Cu_{1.94}S$–ZnS heteronanostructures (a). Synthetic routes for preparation of different hexagonal prism $Cu_{1.94}S$–ZnS heteronanostructures (b). Adapted with permission from ref. 35 Copyright© 2012 WILEY-VCH Verlag GmbH & Co. KGaA, Weinheim.
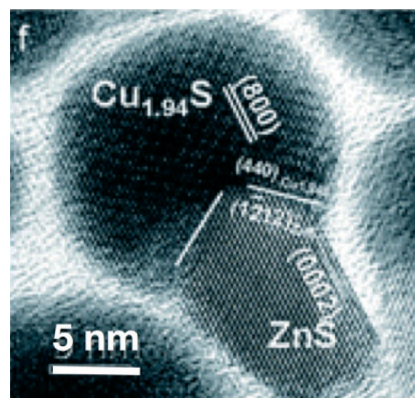

Fig. 10 A $Cu_{1.94}S$–ZnS heteronanostructure. Adapted from ref. 34 with permission from The Royal Society of Chemistry.

particles, and, consequently, the hybrid structures with ZnS were formed only above a certain copper amount in the reaction solution. Below this amount, cubic copper-doped ZnS was formed whereas the ZnS phase which was found within the hybrid nanostructures had a hexagonal wurtzite structure and did not contain copper dopant atoms. The authors assume that the dissolution of Zn ions in $Cu_{1.94}S$ nanocrystals is the first step in the formation of the hybrid nanocrystals.

$Cu_{1.94}S$–CdS and $Cu_{1.94}S$–$Zn_xCd_{1-x}S$ nanodisc heterostructures were synthesized by Regulacio et al. in 2011.[37] The resulting nanodiscs exhibit a hexagonal shape and are composed of copper sulphide and CdS (or $Zn_xCd_{1-x}S$) regions (Fig. 11). Because of the conservation of the original hexagonal shape of the copper sulphide particles formed in the beginning of the synthesis the authors assume cation exchange to be the reaction mechanism for the generation of the nanostructures.

The formation of PbS–Cu_2S hybrid nanorods was reported by Zhuang et al.[38] in 2012. Addition of a Pb precursor to djurleite copper sulphide seeds resulted in the formation of cubic PbS nanorods attached to the hemispheres of copper sulphide with a chalcocite structure (Fig. 12). Thus, a phase transformation occurred in the copper sulphide particles during the formation of the PbS nanorods. The authors assume that the formation of PbS seeds is a consequence of
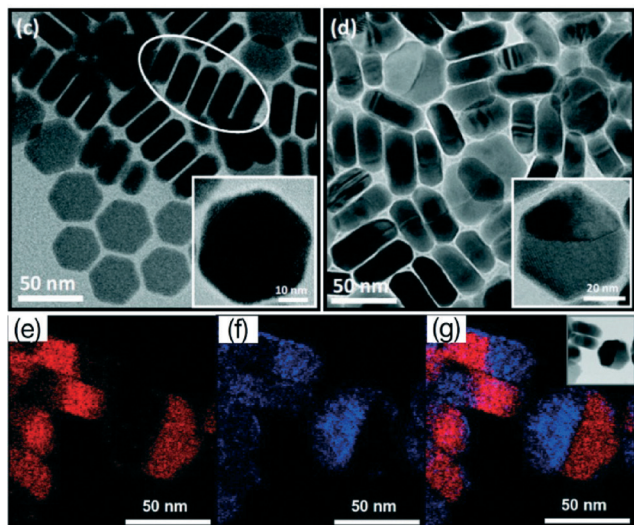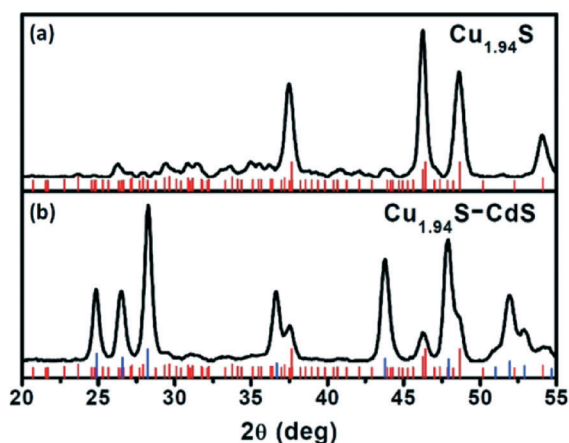

Fig. 12 TEM images of (a) $Cu_{1.94}S$ and (b) Cu_2S–PbS heteronanostructures. Below the TEM images, a scanning TEM (STEM) image and the high resolution element mapping of Cu_2S–PbS heteronanostructures are shown. The scale bars are all 40 nm. Adapted from ref. 38 with permission from The Royal Society of Chemistry.

Fig. 11 XRD patterns of (a) $Cu_{1.94}S$ and (b) $Cu_{1.94}S$–CdS nanodiscs. TEM images of (c) $Cu_{1.94}S$ and (d) $Cu_{1.94}S$–CdS nanodiscs. EFTEM images of $Cu_{1.94}S$–CdS nanodiscs showing the (a) Cu and (b) Cd elemental maps. The energy filtered TEM images are displayed in (e–g). Cu-containing regions are coded red, whereas Cd-containing segments are coded blue. Adapted with permission from *J. Am. Chem. Soc.*, 2011, **133**, 2052–2055. Copyright (2011) American Chemical Society.
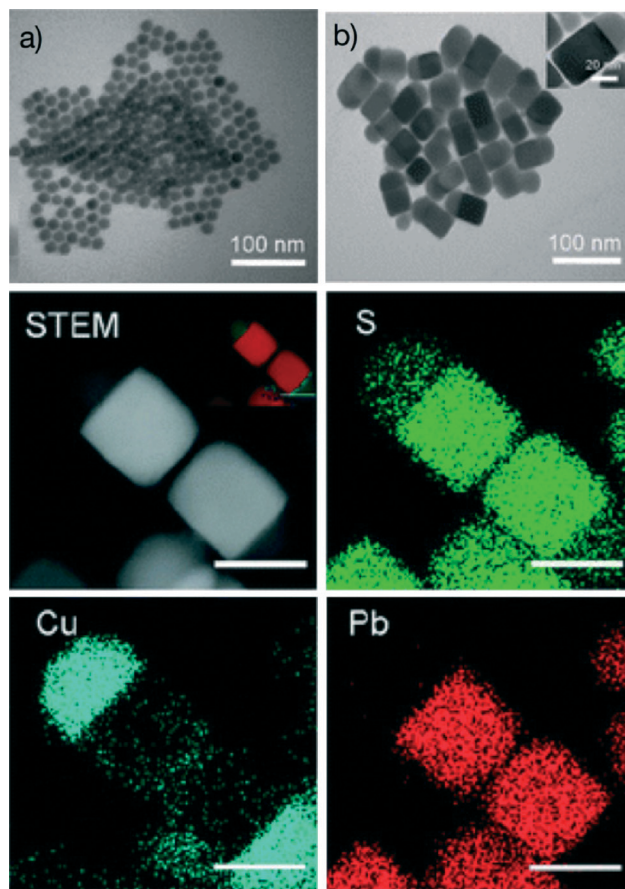
partial cation exchange, while further growth results from the deposition of Pb and S monomers on the surface of these PbS seeds.

A similar growth mechanism based on partial cation exchange and subsequent growth on the surface of the newly formed seeds was reported for the $Cu_{1.94}S$–MnS nanoheterostructures by Zhou et al.[39] MnS formed in this reaction had a wurtzite structure, while control experiments without copper sulphide resulted in the formation of the cubic modification of MnS.

Conclusions

Copper sulphide based hybrid nanocrystals are an interesting class of materials with application potential in solar energy conversion, optoelectronics, and theranostics. Furthermore, copper sulphide seeds can be used to synthesize and control the shape of materials which are interesting for many applications, especially in solar energy conversion. Copper sulphide based hybrid nanocrystals can be synthesized starting with seeds exhibiting different crystallographic structures. The most commonly used are monoclinic djurleite seeds; however,

roxbyite and chalcocite seeds were also reported. Further investigations will be necessary to find out if the crystallographic structure of the seeds can influence the growth process of the hybrid nanocrystals. Also the influence of the shape of the seeds has not been studied yet. Preparation of hybrid nanocrystals using seeds with different shapes could open up new possibilities of shape control of such heteronanostructures. Furthermore, the reaction mechanisms suggested in different studies differ from one another and need to be studied in more detail, e.g., by in situ techniques. A deeper understanding of the underlying growth process will enable more precise control of the properties of the hybrid nanostructures and a more efficient exploitation of their application potential.

Notes and references

1 C. B. Murray, C. R. Kagan and M. G. Bawendi, Annu. Rev. Mater. Sci., 2000, 30, 545–610.

2 K. L. Sowers, B. Swartz and T. D. Krauss, Chem. Mater., 2013, 25, 1351–1362.

3 J. H. Han, S. Lee and J. Cheon, Chem. Soc. Rev., 2013, 42, 2581–2591.

4 J. Park, J. Joo, S. G. G. Kwon, Y. Jang and T. Hyeon, Angew. Chem., Int. Ed., 2007, 46, 4630–4660.

5 P. Samokhvalov, M. Artemyev and I. Nabiev, Chem. – Eur. J., 2013, 19, 1534–1546.

6 D. Aldakov, A. Lefrançois and P. Reiss, J. Mater. Chem. C, 2013, 1, 3756–3776.

7 J. Kolny-Olesiak and H. Weller, ACS Appl. Mater. Interfaces, 2013, 5, 12221–12237.

8 E. Witt and J. Kolny-Olesiak, Chem. – Eur. J., 2013, 19, 9746–9753.

9 D. V. Talapin, J.-S. Lee, M. V. Kovalenko and E. V. Shevchenko, Chem. Rev., 2010, 110, 389–458.

10 A. Chen and S. Chatterjee, Chem. Soc. Rev., 2013, 42, 5425–5438.

11 D. Wang and Y. Li, Adv. Mater., 2011, 23, 1044–1060.

12 B. Kim, M. Hackett, J. Park and T. Hyeon, Chem. Mater., 2014, 26, 59–71.

13 L. Carbone and P. D. Cozzoli, Nano Today, 2010, 5, 449–493.

14 R. Costi, A. E. Saunders and U. Banin, Angew. Chem., Int. Ed., 2010, 49, 4878–4897.

15 P. D. Cozzoli, T. Pellegrino and L. Manna, Chem. Soc. Rev., 2006, 35, 1195–1208.

16 C. de Mello Donegá, Chem. Soc. Rev., 2011, 40, 1512–1546.

17 L. Chen, Y.-B. Chen and L.-M. Wu, J. Am. Chem. Soc., 2004, 126, 16334–16335.

18 Y. Wu, C. Wadia, W. Ma, B. Sadtler and P. Alivisatos, Nano Lett., 2008, 8, 2551–2555.

19 H. Zhang, Y. Zhang, J. Yu and D. Yang, J. Phys. Chem. C, 2008, 112, 13390–13394.

20 W. P. Lim, C. T. Wong, S. L. Ang, H. Y. Low and W. S. Chin, Chem. Mater., 2006, 18, 6170–6177.

21 Y. Wang, Y. Hu, Q. Zhang, J. Ge, Z. Lu, Y. Hou and Y. Yin, Inorg. Chem., 2010, 6601–6608.

22 M. Kruszynska, H. Borchert, A. Bachmatiuk, M. H. Rümmeli, B. Buechner, J. Parisi and J. Kolny-Olesiak, ACS Nano, 2012, 6, 5889–5896.

23 I. Kriegel, J. Rodríguez-Fernández, E. Da Como, A. A. Lutich, J. M. Szeifert and J. Feldmann, Chem. Mater., 2011, 23, 1830–1834.

24 S. T. Connor, C.-M. Hsu, B. D. Weil, S. Aloni and Y. Cui, J. Am. Chem. Soc., 2009, 131, 4962–4966.

25 M. Kruszynska, H. Borchert, J. Parisi and J. Kolny-Olesiak, J. Am. Chem. Soc., 2010, 132, 15976–15986.

26 J.-Y. Chang and C.-Y. Cheng, Chem. Commun., 2011, 47, 9089–9091.

27 M. Kruszynska, H. Borchert, J. Parisi and J. Kolny-Olesiak, J. Nanopart. Res., 2011, 13, 5815–5824.

28 X. Lu, Z. Zhuang, Q. Peng and Y. Li, CrystEngComm, 2011, 13, 4039–4045.

29 Q. Li, L. Zhai, L. Zou, X. Huang, L. Zhang, Y. Yang, X. Chen and S. Huang, Nanoscale, 2013, 5, 1638–1648.

30 C. Coughlan, A. Singh and K. Ryan, Chem. Mater., 2013, 25, 653–661.

31 W. Zhang, L. Zhai, N. He, C. Zou, X. Geng, L. Cheng, Y. Dong and S. Huang, Nanoscale, 2013, 5, 8114–8121.

32 H.-C. Liao, M.-H. Jao, J.-J. Shyue, Y.-F. Chen and W.-F. Su, J. Mater. Chem. A, 2013, 1, 337.

33 L. Yi, A. Tang, M. Niu, W. Han, Y. Hou and M. Gao, CrystEngComm, 2010, 12, 4124.

34 F. Huang, X. Wang, J. Xu, D. Chen and Y. Wang, J. Mater. Chem., 2012, 22, 22614.

35 S.-K. Han, M. Gong, H.-B. Yao, Z.-M. Wang and S.-H. Yu, Angew. Chem., Int. Ed., 2012, 51, 6365–6368.

36 H. Ye, A. Tang, L. Huang, Y. Wang, C. Yang, Y. Hou, H. Peng, F. Zhang and F. Teng, Langmuir, 2013, 29, 8728–8735.

37 M. D. Regulacio, C. Ye, S. H. Lim, M. Bosman, L. Polavarapu, W. L. Koh, J. Zhang, Q.-H. Xu and M.-Y. Han, J. Am. Chem. Soc., 2011, 133, 2052–2055.

38 T.-T. Zhuang, F.-J. Fan, M. Gong and S.-H. Yu, Chem. Commun., 2012, 48, 9762–9764.

39 J. Zhou, F. Huang, J. Xu and Y. Wang, CrystEngComm, 2013, 15, 4217.

40 W. Han, L. Yi, N. Zhao, A. Tang, M. Gao and Z. Tang, J. Am. Chem. Soc., 2008, 130, 13152–13161.

41 H. J. Fan, P. Werner and M. Zacharias, Small, 2006, 2, 700–717.

42 Y.-Z. Long, M. Yu, B. Sun, C.-Z. Gu and Z. Fan, Chem. Soc. Rev., 2012, 41, 4560–4580.

43 S. Hoshino, Solid State Ionics, 1991, 48, 179–201.

44 K. Wakamura and I. Tsubota, Solid State Ionics, 2000, 130, 305–312.

45 L.-W. Wang, Phys. Rev. Lett., 2012, 108, 085703.

46 S.-H. Choi, E.-G. Kim and T. Hyeon, J. Am. Chem. Soc., 2006, 128, 2520–2521.

47 L. Yi, Y. Liu, N. Yang, Z. Tang, H. Zhao, G. Ma, Z. Su and D. Wang, Energy Environ. Sci., 2013, 6, 835–840.

48 P. K. Jain, L. Amirav, S. Aloni and P. Alivisatos, J. Am. Chem. Soc., 2010, 132, 9997–9999.

49 Y. Zhao and C. Burda, Energy Environ. Sci., 2012, 5, 5564–5576.

50 D. Pan, L. An, Z. Sun, W. Hou, Y. Yang, Z. Yang and Y. Lu, J. Am. Chem. Soc., 2008, 130, 5620–5621.